

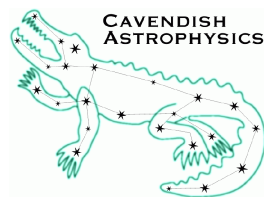
MRO FTT/NAS & FLC

Derived Requirements

MRO-TRE-CAM-0000-0101

The Cambridge FTT Team

rev 1.0
31 August 2010



Cavendish Laboratory
Madingley Road
Cambridge CB3 0HE
UK

Change Record

Revision	Date	Authors	Changes
0.1	2010-06-08	JSY	Initial version
	2010-06-23	CAH	Initial drafts of Image Quality and Zero-point stability sections
	2010-07-13	CAH	Additional content on Image Quality and Zero-point stability sections
	2010-07-15	ADR	Added zoom layout; other minor additions
	2010-07-18	CAH	Typos and minor corrections
	2010-07-18	ADR	Expanded on description and analysis of Zoom layout where needed
0.2	2010-08-06	JSY	Merged sections from CAH/ADR, DFB, JSY
0.3	2010-08-06	JSY	Correction to pixel scale section
0.4	2010-08-24	JSY	Inserted updates from received on 2010-08-20 from CAH, DFB. Added closed-loop bandwidth section. Added thermal management section from MF
0.5	2010-08-25	JSY	Added bibliography. Minor edits
1.0	2010-08-31	JSY	Corrections from DFB and MF

Objective

To present the derived requirements for the FTT/NAS and FLC systems.

Scope of this document

This document outlines how the derived requirements were calculated from the top-level requirements specified by MRO, including any assumptions made about the design of the FTT/NAS and FLC, and presents the results of the calculations.

Reference documents

- RD1** Technical Requirements: Fast Tip-Tilt/Narrow-field Acquisition System (INT-403-ENG-0003) – rev 2.2, May 20th 2010
- RD2** Technical Requirements: First Light Camera (INT-403-TSP-0107) – rev 1.0, May 20th 2010
- RD3** Technical Requirements: Unit Telescopes for the MRO Interferometer (INT-403-TSP-0003) – October 27th 2006

Contents

1	Introduction	4
2	Conceptual Design Assumptions	4
3	Pixel Scale	4
3.1	Top-level requirements	4
3.2	Design assumptions	5
3.3	Derived requirements	5
4	FTT mode subframe size	5
4.1	Top-level requirements	5
4.2	Design assumptions	5
4.3	Derived requirements	6
5	Image Quality	6
5.1	Top-level requirements	6
5.2	Design assumptions	7
5.3	Derived requirements	7
6	Stability of Tip-tilt zero point	10
6.1	Top-level requirements	10
6.2	Design assumptions	11
6.3	Derived requirements	11
7	Thermal Management	13
7.1	Top-level requirements: FTT/NAS	13
7.1.1	Environmental Conditions	13
7.1.2	Heat dissipation	13
7.1.3	Power consumption	13
7.2	Design assumptions: FTT/NAS	13
7.3	Derived requirements: FTT/NAS	14
7.3.1	Top-level requirements: FLC	15
7.4	Design assumptions: FLC	16
7.5	Derived requirements: FLC	16
8	Closed-loop Bandwidth	17
8.1	Top-level requirements	17
8.2	Design assumptions	17
8.3	Derived requirements	17

9	Limiting Sensitivity	18
9.1	Top-level requirements	18
9.2	Design assumptions	18
9.3	Derived requirements	18
10	Dynamic Range	20
10.1	Top-level requirements	20
10.2	Design assumptions	20
10.3	Derived requirements: FTT	20
11	Derived requirements: NAS and FLC	21

1 Introduction

This document specifies “derived requirements” and error budgets which apply to particular components of the FTT/NA and FLC systems. These have been calculated from the top-level requirements specified in RD1 and RD2, on the basis of a minimal set of assumptions about the conceptual designs of the FTT/NAS and FLC respectively. The calculations are presented in outline form, with references to published papers where appropriate.

2 Conceptual Design Assumptions

In order to quantify the derived requirements it is necessary to make certain assumptions about the conceptual design of the FTT/NA and FLC systems. The main assumptions, applied in several of the subsequent sections, are as follows:

- we assume that a single camera is used for target acquisition and fast tip-tilt sensing and that the same focusing optic(s) are used to image the target onto the camera in all operating modes;
- we assume that the camera is an electron-multiplying CCD (EMCCD) with 512×512 pixels and a read noise of 50 electrons RMS.

Further assumptions are described in the sections below to which they apply.

3 Pixel Scale

In this section we present the top-level and derived requirements on the image pixel scale for the FTT/NAS and FLC.

3.1 Top-level requirements

For the FLC, there is a top-level requirement on the pixel scale:

FLC-UR2-02 : The pixel scale shall be between 0.15 and 0.25 arcsec per pixel

For the FTT/NAS, the pixel scale is a derived requirement. The following top-level requirements are relevant to the choice of pixel scale:

- The field-of-view of each captured image frame in acquisition mode shall be at least $60 \text{ arcsec} \times 60 \text{ arcsec}$, with a goal of $100 \text{ arcsec} \times 100 \text{ arcsec}$
- Given assumptions 1–8 (see RD1), the rms residual two-axis tip-tilt (i.e. the quadrature sum of the tip and tilt residuals for the tip-tilt reference object) when the system is operating in tip-tilt mode shall not exceed 0.060 arcsec for tip-tilt reference objects brighter than $V = 16$. The residual referred to here is total residual of the atmospheric disturbances, the Unit Telescope mount errors and the wind shake errors (see Sec. 2.6.3 of RD3).

In the following subsections we use these constraints to determine the allowed range of pixel scale for the FTT/NAS.

3.2 Design assumptions

We assume that a single camera is used for target acquisition and fast tip-tilt sensing and that the same focusing optic(s) are used to image the target onto the camera in all operating modes. Hence the pixel scale will be identical for acquisition and fast tip-tilt modes.

In order to have sufficient field-of-view for acquisition, the CCD camera is assumed to have 512×512 pixels.

We further assume that the best seeing in which the FTT/NAS performance requirements must be satisfied shall be 0.7 arcsec FWHM.

3.3 Derived requirements

The pixel scale for the FTT/NAS shall be between 0.12 and 0.2 arcsec per pixel. The derivation is as follows.

A pixel scale of $60/512 = 0.12$ arcsec/pix or greater is needed to realise the *requirement* of $60 \text{ arcsec} \times 60 \text{ arcsec}$ acquisition field-of-view using a 512×512 pixel CCD (this must be increased to 0.195 arcsec/pix to meet the 100 arcsec FOV *goal*).

We cannot use an arbitrarily coarse pixel scale since this will not allow the tip-tilt to be sensed with sufficient accuracy to meet the 0.060 arcsec residual requirement. The difficulty of centroiding accurately will be exacerbated by the objective point position not being fixed at the centre or edge of a CCD pixel.

To ensure accurate centroiding, we require a minimum of 2.5 pixels across the short-exposure image FWHM. Following [Roddier et al. \[1991\]](#), we assume that the FWHM of the short-exposure speckle cloud will be approximately $\sqrt{2}$ smaller than the long-exposure seeing FWHM, and hence be 0.5 arcsec FWHM in the best (i.e. worst-case) seeing. Hence the maximum pixel scale is $0.5/2.5 = 0.2$ arcsec/pixel.

4 FTT mode subframe size

In this section we derive the minimum dimensions of the CCD subframe that is read out in the fast tip-tilt mode of the FTT/NAS. The FLC will not do fast tip-tilt correction and hence does not require fast readout of small subframes.

4.1 Top-level requirements

The following FTT/NAS top-level requirements are relevant:

- the field-of-view in fast tip-tilt mode shall be at least $3 \text{ arcsec} \times 3 \text{ arcsec}$;
- use of an off-axis object up to 10 arcsec from the science target as the tip-tilt reference object;
- the system is expected to run uninterrupted in fast tip-tilt mode for a maximum of 300 s (Sec. 5.10.2 of RD1).

Note that the top-level requirement for dispersion-offset guiding is *not* relevant to the choice of subframe size, since the change in the dispersion offset over 300 s will be at most 0.05 arcsec.

4.2 Design assumptions

The system must allow for field rotation (inherent with any non-equatorial telescope mount), which manifests itself as the image of the sky seen by the FTT camera rotating about the telescope pointing centre at a rate that depends on the pointing direction within the field of regard. When using an off-axis tip-tilt reference object, the

unit telescope pointing centre will be the tip-tilt zero point (the telescope having been commanded to point to the science target) therefore field rotation will cause the image of the tip-tilt reference object to follow a circular trajectory centred on the tip-tilt zero point.

We assume that it will not be possible to change the location of the CCD subframe without interrupting fast tip-tilt mode, however briefly. Hence the system will be designed to use a subframe whose location is fixed for the duration of fast tip-tilt mode, the subframe location being optimally selected based on advance knowledge of the off-axis offset as a function of time.

When fast tip-tilt mode is activated, the CCD camera will be configured to read out a subframe positioned such that a 3 arcsec-square box centred on the tip-tilt reference object is initially at one edge of the subframe and subsequently moves towards the opposite edge. The subframe size must be large enough to accommodate the motion of of the reference object over the maximum observation duration of 300 s.

4.3 Derived requirements

The worst-case field rotation rate $\frac{d\theta}{dt}$ is 40 arcsec/sec, for a target at declination +26 degrees and hour angle +4.5 hours. The maximum arc length traversed by the image of the reference object at separation $r = 10$ arcsec, in $\Delta T = 300$ s, is therefore $r \frac{d\theta}{dt} \Delta T = 0.6$ arcsec. In the worst case this will be parallel to an edge of the subframe, hence the fast tip-tilt mode subframe dimension must be at least $3 + 0.6 = 3.6$ arcsec.

For the range of pixel scales derived in Sec. 3, this subframe size corresponds to between 18 and 30 pixels.

5 Image Quality

5.1 Top-level requirements

There is no explicit top-level requirement on image quality for the FTT/NA system. However, implicit requirements on image quality arise from three other needs that have been placed on the FTT/NA system. These are:

1. that in acquisition mode the system provide rough estimates of the image FWHM for the purposes of system optimisation;
2. that the field of view in acquisition mode be at least as large as $\pm 30''$;
3. that in FTT mode, it be possible to utilise an off-axis guide star up to $10''$ distant from the science object.

The third of these is clearly the most demanding, and so we have choosen to require that the image of a point source delivered by the FTT/NA system within a $20'' \times 20''$ window centred on the system optical axis have a 50% encircled energy diameter no greater than the width of a single detector pixel ($16\mu\text{m}$). By way of comparison, a perfect Airy pattern has a FWHM approximately equal to its 50% encircled energy diameter.

Since the derived requirement for the FTT/NA pixel scale (see section 3 above) demands a pixel scale much smaller than the $0.7''$ long-exposure image FWHM expected under optimum seeing conditions (i.e. $r_0 = 14$ cm at 500 nm), it is clear that an amount of static off-axis image smearing ≤ 1 pixel will have only an insignificant impact on the performance of acquisition or autoguiding.

There is an explicit top-level requirement on image quality for the FLC. This is that it deliver image quality of at least one second of arc FWHM over a $60'' \times 60''$ field of view. This is a less stringent requirement than the implicit FTT/NA requirement outlined above, and so it is the former derived requirement that we will focus on below.

5.2 Design assumptions

In the following subsection we outline the derived requirements, on a component-by-component basis, for four possible conceptual layouts for the FTT/NA system. These are:

1. a layout using an off-axis parabola for focusing the UT beam, and a single fold mirror: hereafter we will refer to this as the OAP (“off-axis parabola”) configuration (see Fig. 1(a));
2. a layout using a transmissive achromatic lens for focusing the UT beam, and a single fold mirror: hereafter we will refer to this as the DT (“direct transmissive”) configuration (see Fig. 1(b));
3. an alternative layout using a transmissive achromatic lens optic for focusing the UT beam, but with two fold mirrors to feed the beam to the detectors. Hereafter we will refer to this as the DLT configuration (Fig. 1(c));
4. a layout using a fast primary lens, a single fold mirror and a secondary lens, with a negative focal length, close to the detector. This allows an effective focal length that is larger than the physical distance the beam has travelled. Hereafter we will refer to this as the “Zoom” configuration (see Fig. 1(d)).

In all four of these configurations the collimated beam from M3 will be intercepted by a dichroic which reflects the wavelengths to be sent to the FTT/NA system (at an angle of incidence of 15°) and which transmits the remaining longer wavelengths to the beam relay system. The reflected beam will then be focused and thereafter sent to the detector via either one (for the OAP, DT and Zoom configurations) or two (for the DLT configuration) plane mirrors. The Zoom configuration has, in addition, a negative focal length lens close to the detector. The first two of these layouts utilise focusing optics with very similar focal lengths (1600 mm and 1525 mm respectively) but locate the detector at rather different places on the Nasmyth optical table, whereas the final two layouts allow for all of the elements of the optical train to be located close to each other, but at the expense of needing either one additional reflective or focussing element in the optical train.

5.3 Derived requirements

In this subsection we present a tabular summary of the tolerances on each of the optical elements for the OAP, DL, DLT and Zoom layouts that give rise to a 50% encircled energy diameter equal to the width of one detector pixel. Because the field of view for fast tip-tilt sensing must be at least as large as $\pm 10''$, we have assumed observations of a target at the edge of a ± 10 second of arc field of view.

Each optical component has, in principle, six degrees of freedom: three translational degrees of freedom and three angular degrees of freedom. Hereafter we shall use the co-ordinate z to denote displacements parallel to the optical axis of an optical element (or perpendicular to its surface, for flat components), and x and y to represent displacements perpendicular to this. We define the x direction to be that which is perpendicular to the Nasmyth optical table.

The values in table 1 were obtained by constructing a ZEMAX model of each layout and perturbing each element in one degree of freedom at a time until the 50% encircled energy diameter increased above one pixel i.e. $16 \mu\text{m}$. The magnitude of the displacements required for this to occur are what is shown in table 1. Each element was returned to its intended location before another degree of freedom or another optical element was disturbed. An observing wavelength of 600 nm was assumed. The reader should note that the FTT/NA system will be required to operate either using light between 600 and 1000 nm or between 350–600 nm. We anticipate having to use an achromatic doublet or triplet for the lens-based layouts.

Table 1 does not present an error budget for the allowed displacements, but rather gives an assessment as to which optical components are more tolerant of displacements (and for which co-ordinates), and whether of not any one of the four conceptual layouts might be preferred because it is more tolerant of displacements of its components from their nominal positions. This last point is worth highlighting: because the values in the table

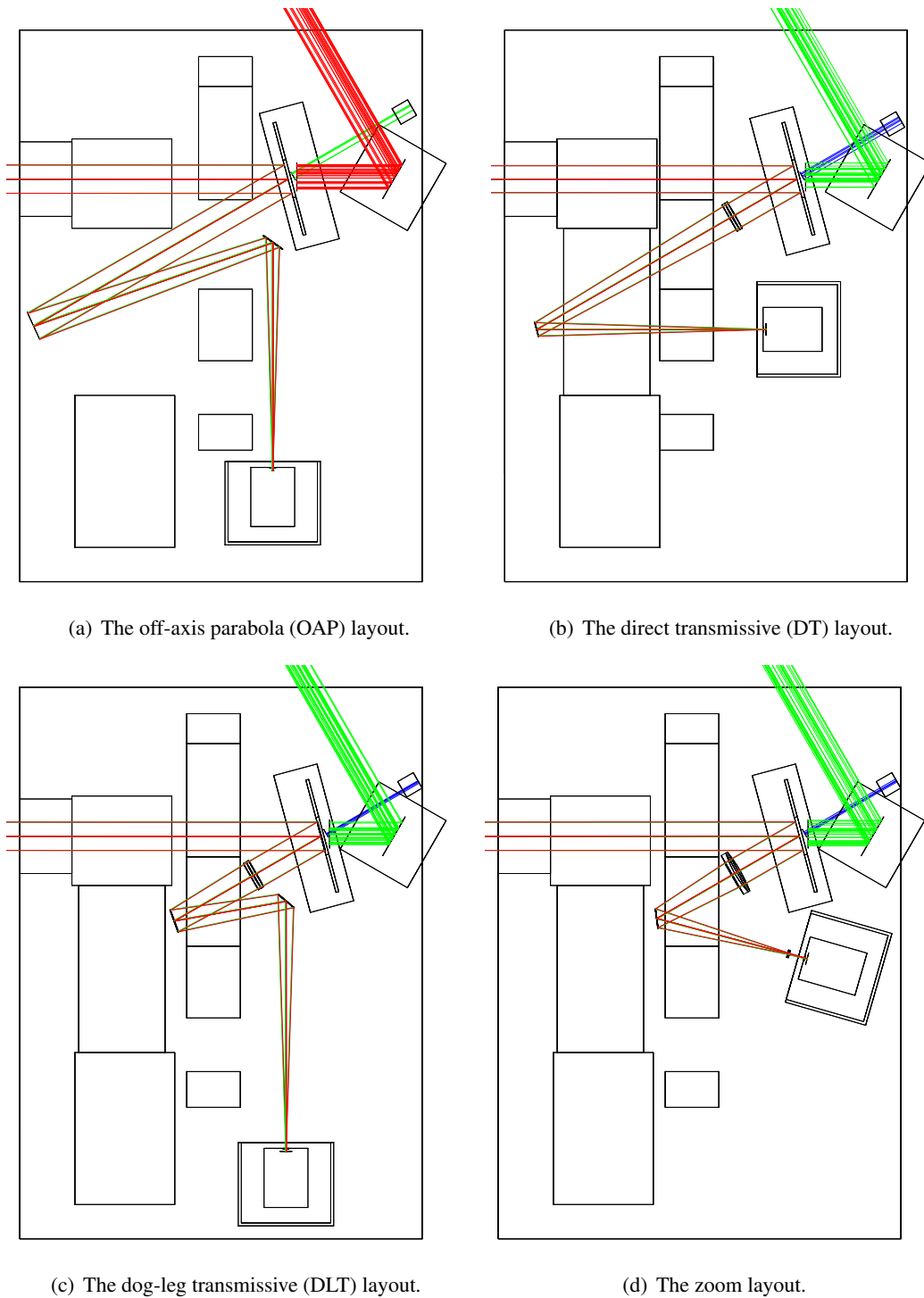


Figure 1: Summary of layouts under consideration. In all cases, the collimated beam from the telescope tertiary mirror enters horizontally from the left.

Item	degree of freedom	OAP	DT	DLT	Zoom
Dichroic	δx				
“	δy				
“	δz	> 5 mm	> 5 mm	> 5 mm	> 5 mm
“	$\delta\theta_x$	0.053°	0.34°	0.37°	0.14°
“	$\delta\theta_y$	0.053°	0.34°	0.37°	0.14°
“	$\delta\theta_z$				
Focus optic 1	δx	> 5 mm	> 5 mm	> 5 mm	> 5 mm
“	δy	> 5 mm	> 5 mm	> 5 mm	> 5 mm
“	δz	0.38 mm	0.35 mm	0.35 mm	0.12 mm
“	$\delta\theta_x$	0.10°	0.93°	0.93°	0.75°
“	$\delta\theta_y$	0.10°	0.93°	0.93°	0.75°
“	$\delta\theta_z$				
Fold mirror 1	δx				
“	δy				
“	δz	0.23 mm	0.22 mm	0.17 mm	0.065 mm
“	$\delta\theta_x$	0.9°	0.8°	0.65°	0.33°
“	$\delta\theta_y$	1.0°	1.6°	1.9°	0.25°
“	$\delta\theta_z$				
Focus optic 2	δx	n/a	n/a	n/a	4 mm
“	δy	n/a	n/a	n/a	4 mm
“	δz	n/a	n/a	n/a	0.18 mm
“	$\delta\theta_x$	n/a	n/a	n/a	4.5°
“	$\delta\theta_y$	n/a	n/a	n/a	4.5°
“	$\delta\theta_z$	n/a	n/a	n/a	
Fold mirror 2	δx	n/a	n/a		n/a
“	δy	n/a	n/a		n/a
“	δz	n/a	n/a	0.22 mm	n/a
“	$\delta\theta_x$	n/a	n/a	0.77°	n/a
“	$\delta\theta_y$	n/a	n/a	1.2°	n/a
“	$\delta\theta_z$	n/a	n/a		n/a
CCD	δx				
“	δy				
“	δz	0.38 mm	0.35 mm	0.35 mm	0.3 mm
“	$\delta\theta_x$	> 5°	> 5°	> 5°	> 5°
“	$\delta\theta_y$	> 5°	> 5°	> 5°	> 5°
“	$\delta\theta_z$				

Table 1: Individual element tolerance in position and angle that lead to a 50% encircled energy diameter of greater than one pixel (16 μm) for the OAP, DL, DLT and zoom layouts. The focal lengths assumed were 1600 mm, 1525 mm, 1525 mm and 1315 mm respectively. The effective 1315 mm focal length for the Zoom layout is made up of two lenses, focal lengths of 800 mm and -100 mm.

represent the maximum allowable displacements from the nominal locations of the components, they can be used to derive the *absolute* positioning accuracy needed when the optical elements are first installed.

The data presented in table 1 provide a number of different insights that are worth highlighting. These relate both to the positioning of individual components in each optical train, but also to possible preferences between the four layouts investigated.

1. **Preferences between layouts:** it is immediately apparent that the allowable displacements for the OAP layout are generally stricter than the Zoom layout, which in turn is stricter than the DT and DLT lens-based layouts. The OAP layout has a six-fold more stringent angular installation tolerance ($\delta\theta_{x,y}$) on the dichroic as compared to the lens-based layouts and is roughly 3 times more sensitive than the zoom layout. This is because the field of view of an off-axis parabola degrades when it is used at any field angle other than that which it was designed for. Similarly, for the Zoom layout, the compound system formed by the two lenses has a narrower field of view than a single lens.

Because of this narrow field of view, the OAP layout also has a strict angular installation tolerance on the off-axis parabola itself. However, the angular installation tolerance of the first lens of the Zoom layout has a similar value to that of the other lens based layouts. This difference is because tilting the single lens has a much smaller effect on the image quality than changing the input angle of the beam; the field of view of a single lens is quite wide.

2. **Positional tolerances:** the positional tolerances on the optical elements of all four layouts are relatively benign. There is little need to accurately locate the optical elements in the x and y directions, whereas in the z direction, the tolerances are directly related to the depth of field of the focusing element. This is typically at the 300-400 micron level and so as long as there is a degree of freedom to focus the detector after the initial install of the optical elements, it should be relatively straightforward to satisfy an error budget based on these numbers.
3. **Angular tolerances:** the angular tolerances on the optical elements are similarly benign, and are essentially related to either the field of view of the focus optic, or the ability to steer the focused beam so that it lands on the detector. This latter requirement can be easily met if the detector is positioned in the x and y directions after the other optical elements have been installed. The 8-fold smaller field of view of the off-axis parabola is the most important feature to note.
4. **CCD location:** if the detector head can be adjusted in the x , y and z directions, then small errors in the positions and orientations of the other optical elements can easily be corrected.

In summary, the image quality needed for the FTT/NA and FLC systems appears to require relatively imprecise and inaccurate positioning of the elements in the optical train. The majority of the critical tolerances are those associated with obtaining a good enough focus — the typical depth of field is approximately $\pm 350 \mu\text{m}$. If the OAP (or Zoom) layouts are used, then the dichroic must be aligned with respect to the optical train to better than roughly one (three) minute(s) of arc. The folding mirror between the powered elements of the Zoom layout must also be aligned to a similar degree of accuracy if the Zoom layout is used.

6 Stability of Tip-tilt zero point

6.1 Top-level requirements

The top-level requirement on the tip-tilt zero point stability is that any changes due, for example, to tilt or position drifts of the optical components on the Nasmyth optical table, not exceed 0.015 seconds of arc (when referred to the sky). This assumes ambient temperature changes of at most 5 °C, with any changes occurring at a rate of no more than 1.5 °C/hour. This stability constraint must be met for the whole night after the tip-tilt zero point has been set at the start of the night.

The equivalent requirement for the FLC is that any image motion induced by temperature changes of up to 5 °C correspond to no greater than 1 second of arc on the sky. This is close to 70 times less stringent a requirement than the FTT/NA requirement and so as in section 5 we concentrate below solely on the needs of the FTT/NA system.

6.2 Design assumptions

Following section 6.4 of the FTT/NA requirements document, we have assumed that the Nasmyth optical table presents a perfectly stable platform on which the components considered in our possible conceptual designs are mounted.

We present in the following subsection our derived stability requirements, on a component-by-component basis, for the same four conceptual layouts for the FTT/NA system (OAP, DT, DLT and Zoom). However, the data are not a simple tabulation of the sensitivity of the zero-point to displacements of each optical element but instead are a version of a full system error budget where maximum permissible displacements in angle and position have been allocated to each component such that their rms total is consistent with both the top level stability requirement and the image quality budget.

The primary contributors to motion of the FTT/NA system zero-point will be shears (i.e. motions in the x and y directions) or tilts of the optical components. It is usually more difficult to constrain the tilt of an optic as compared to its position, and so for the budget presented below we have allocated $\sqrt{(2/3)}$ of the budget to uncontrolled tilts that move the zero point and $\sqrt{(1/3)}$ to uncontrolled shears, and for each component, the budget has been divided equally between contributions that move the zero-point in the x and y directions.

6.3 Derived requirements

Table 2 shows the error budgets for the maximum allowable component displacements that meet the top-level zero-point stability budget for the OAP, DL, DLT and Zoom layouts. The reader should note that these values assume the optical elements have been initially installed at their nominal positions and been oriented perfectly. This is unlikely to be strictly true, but the data presented are likely to be sufficiently accurate as long as the elements have been installed well enough to meet the image quality requirements of the FTT/NA system.

The elements of table 2 provide a number of different insights worth highlighting.

1. **Preferences between layouts:** it is clear that all the layouts present very challenging requirements on the optical element stability. Perhaps the only significant difference is the very strict angular tolerance on permissible rotations of the focusing optics about the x , y and x axes that the use of an off-axis parabola entails.
2. **Positional tolerances:** the positional tolerances on the optical elements of all four layouts are very severe. Instabilities in the x and y locations of the focusing optics relative to the detector focal plane lead to zero-point shifts, as do transverse motions of the fold mirrors. The order of magnitude of the allowed displacements is at the half micron level. Motions along the beam propagation direction are primarily associated with the depth of field of the detector.
3. **Angular tolerances:** the angular tolerances on the optical elements are similarly challenging. Angular displacements of the optical components lead directly to image plane motions, and so most of the optical elements in all the layouts need to be stable in angle at roughly the 0.05'' level.
4. **CCD location:** unlike the case for image quality, motions of the detector perpendicular to the normal to its surface will immediately give rise to zero-point errors. The maximum permissible motions are at the half micron level.

Item	degree of freedom	OAP	DT	DLT	Zoom
Dichroic	δx				
“	δy				
“	δz				
“	$\delta \theta_x$	0.040''	0.052''	0.047''	0.066''
“	$\delta \theta_y$	0.044''	0.058''	0.045''	0.071''
“	$\delta \theta_z$				
Focus optic	δx	0.50 μm	0.47 μm	0.47 μm	0.33 μm
“	δy	0.39 μm	0.42 μm	0.35 μm	0.28 μm
“	δz	270 μm	250 μm	250 μm	80 μm
“	$\delta \theta_x$	0.040''	0.83''	0.75''	0.68''
“	$\delta \theta_y$	0.043''	0.91''	0.70''	0.73''
“	$\delta \theta_z$	0.130''	n/a	n/a	n/a
Fold mirror 1	δx				
“	δy				
“	δz	0.37 μm	0.58 μm	0.59 μm	0.32 μm
“	$\delta \theta_x$	0.057''	0.073''	0.090''	0.084''
“	$\delta \theta_y$	0.098''	0.110''	0.049''	0.10''
“	$\delta \theta_z$				
Focus Optic 2	δx	n/a	n/a	n/a	0.52 μm
“	δy	n/a	n/a	n/a	0.44 μm
“	δz	n/a	n/a	n/a	100 μm
“	$\delta \theta_x$	n/a	n/a	n/a	2.60''
“	$\delta \theta_y$	n/a	n/a	n/a	2.75''
“	$\delta \theta_z$	n/a	n/a	n/a	
Fold mirror 2	δx	n/a	n/a		n/a
“	δy	n/a	n/a		n/a
“	δz	n/a	n/a	0.31 μm	n/a
“	$\delta \theta_x$	n/a	n/a	0.064''	n/a
“	$\delta \theta_y$	n/a	n/a	0.074''	n/a
“	$\delta \theta_z$	n/a	n/a		n/a
CCD	δx	0.50 μm	0.47 μm	0.47 μm	0.42 μm
	δy	0.39 μm	0.42 μm	0.35 μm	0.35 μm
	δz	270 μm	250 μm	250 μm	130 μm
“	$\delta \theta_x$				
“	$\delta \theta_y$				
“	$\delta \theta_z$	2.10''	2.75''	2.32''	3.0''

Table 2: Global error budget for the individual element tolerances in position and angle meet the overall zero-point stability requirement for the OAP, DL, DLT and Zoom layouts.

In summary, the zero-point stability requirement for the FTT/NA system appears to require ultra-stable optical components. The positions and orientations of most of the optical elements must be stable at the sub-micron and sub-arcsecond levels.

7 Thermal Management

7.1 Top-level requirements: FTT/NAS

The appropriate top-level requirements are set out in RD1 on page 17, section 6.1, requirements 57 and 58 and page 20, section 6.5, requirements 67, 68 and 69. These specify the following:

7.1.1 Environmental Conditions

(57) Components of the FTT system on the optical table shall operate over a temperature range of $-5\text{ }^{\circ}\text{C}$ to $20\text{ }^{\circ}\text{C}$ and relative humidity (RH) between 10% and 70%. It is a goal that the operating temperature range is extended down to $-10\text{ }^{\circ}\text{C}$ and the relative humidity range extended up to 90%. Components of the FTT system in the allocated electronics housing shall be capable of operating within the temperature range $+10\text{ }^{\circ}\text{C}$ to $+40\text{ }^{\circ}\text{C}$.

(58) The survival conditions for all components are $-25\text{ }^{\circ}\text{C}$ to $+40\text{ }^{\circ}\text{C}$ and RH 5% to 95%.

7.1.2 Heat dissipation

(67) Wherever possible, components dissipating significant power should be located in the UT electronics housing.

(68) The external surface of any components of the FTT/NA system located on the UT optical table shall be within $2\text{ }^{\circ}\text{C}$ of the ambient temperature during nighttime observing conditions.

7.1.3 Power consumption

(69) The FTT/NA system excluding the FTTA shall consume no more than 250 W.

7.2 Design assumptions: FTT/NAS

The top level requirements place impossible restrictions on any commercial EMCCD camera operating in the open. Although anecdotal evidence suggests that cameras have been operated at temperatures down to $-5\text{ }^{\circ}\text{C}$ these installations are temporary and have been attended by an operator who decides when conditions become unsuitable or, perhaps more to the point, when conditions become suitable and the camera can be safely switched on after ensuring it is clear of any condensation within.

For operational and camera safety reasons a design decision has been made to place the camera within an enclosure. To prevent overheating and to meet the requirement (68) the enclosure must be insulated and heat must be removed. This concept requires that some further assumptions be made:

- The camera enclosure temperature be controlled to protect the camera and to minimize heat dissipation to the environment when operating at night and to ensure that enclosure surface temperature is within $2\text{ }^{\circ}\text{C}$ of ambient.
- That the camera environment be controlled at all times, even though the camera may not be switched on (this ensures that the camera can be switched on without first having to warm up or dry the enclosure).

- Heat will be removed from the camera and the enclosure by fluid at a controlled temperature and flow rate and exchanged into one of the coolant loops available in the telescope enclosure.

To minimize the increase in outer surface temperature (due to residual heat within the enclosure not removed by the cooling system) the camera enclosure outer surface should have a relatively high emissivity. Also, the cover placed over the Nasmyth table (for physical protection and to shield the table from the cold night sky) should have a similar emissivity.

7.3 Derived requirements: FTT/NAS

Several requirements of the camera enclosure can be derived from the camera operating specifications and the environmental limits:

1. Maximum enclosure internal air temperature: 30 °C
2. Minimum enclosure internal air temperature: 0 °C

The enclosure surface temperature differential with ambient of up to ± 2 °C places a requirement on the camera enclosure such that it must allow for a ΔT between its internal air and the outer surface temperature of up to 3 °C (goal 8 °C) to comply with the minimum ambient temperature of -5 °C (goal -10 °C) and camera operation down to 0 °C within the camera enclosure. That is, if the ambient temperature is at the minimum of the operating range, -5 °C, the outer surface temperature of the camera enclosure must be no higher than -3 °C while the inner air temperature must be no lower than 0 °C.

3. Minimum enclosure internal air/external surface temperature differential that must be accommodated: 3 °C (goal 8 °C)

To protect the camera from condensation forming in the enclosure the dew-point of the air within the enclosure should be 5 °C below the coldest internal component.

4. Enclosure air dew point: coldest enclosure internal component -5 °C

It has been determined from thermal modeling that to ensure that the outer surface temperature of the camera enclosure is within +2 °C of ambient the residual heat, i.e. heat not removed from enclosure by the cooling system must not exceed 5 W. This provides for 3 W of convective heat transfer and 2 W of radiative heat transfer assuming an effective 2-surface combined emissivity factor of 0.54.

5. Enclosure residual heat ≤ 5 W
6. Emissivity of outer surface of enclosure > 0.7

Residual heat from the camera (the heat not removed by the peltier cooling circuit within the camera) must be limited to allow heat exchange with cooling elements within the enclosure without forced airflow. The area of cooling elements must be consistent with the feasible dimensions of the camera enclosure, the thickness of insulation likely to be needed and the maximum temperature allowed within the enclosure. Thermal modeling has shown that up to 18 W can be removed with a coolant temperature 5 °C below ambient without the enclosure air temperature exceeding 30 °C. However only 15 W can be removed from the enclosure when the coolant is at 2 °C and the ambient temperature is -5 °C without the surface temperature exceeding -3 °C.

7. Residual camera heat ≤ 20 W [TBC] (based on likely limitations of removing 15 W by unforced heat exchange with fluid).

	Andor iXON 897		Princeton PRO_EM		Hamamatsu ImageEM C9100-13	
Power supply	PCI bus & PSU		PSU		CCU	
Power consumption	68 W [‡]		140 W		140 W	
Power output			112 W			
Power dissipation	Camera	Electronics Housing	Camera	Electronics Housing	Camera	Electronics Housing
Residual power	12 W [†]	26 W	30 W		20 W	64 W [‡]
Peltier power (max)	30 W	~3 W [†]	50 W [‡]		56 W	
Total Power Diss.	42 W	29 W	80 W	28 W [‡]	76 W	

[†] Estimated from measurement or assumed efficiency.

[‡] Calculated as the difference between the manufacturer-quoted power consumption and “power output.”

Table 3: Power dissipation at the camera and within the EIE-provided electronics housing for each candidate camera. In the table “residual power” refers to the heat dissipated by electronics local to the camera head/EIE electronics housing.

8. Camera enclosure space envelope: arranged to fit potential layouts but expected to be 340 mm wide and 300 mm deep but no more than 350 mm high.

According to requirement (69) the FTT/NA system may consume no more than 250 W. It is clear from the power consumption figures in Table 3 that two of the cameras consume 140 W which would leave only 110 W for the FTT/NAS PC, interfaces and any thermal control hardware. This is likely to be insufficient although it might be achievable with the Andor camera.

In the absence of a complete specification for where the 250 W mentioned in requirement (69) may be dissipated, and considering the maximum dissipation for the Hamamatsu camera controller, it has been assumed that up to 250 W of power dissipation may be required within the EIE electronics housing. Heat dissipated at the camera head is additional to this but most of it is carried away by the cooling circuit. Table 3 also shows the power dissipation for each camera system, including where the power is dissipated. The maximum dissipation within the electronics housing for the camera controller is 64 W (the Hamamatsu camera) suggesting that 186 W would be available for the FTT/NAS PC and any custom interfaces or specific thermal control hardware. A suitable breakdown of power for the FTT CPU and interfaces would be 180 W, leaving up to 70 W for the control of the camera. To accommodate any camera the power consumption allowance would need to be increased to 350 W (180 W for the PC, 140 W for the camera and up to 30 W estimated for additional heat exchanger controls)

9. CPU and interface power dissipation allowance 180 W
10. Camera interface and controller power dissipation allowance 70 W
11. Power consumption allowance 350 W (waiver to be sought if necessary)

7.3.1 Top-level requirements: FLC

The appropriate top-level requirements are set out in RD2, section 2.2, page 5, requirements 16 to 18:

FLC-UR2-16: Environmental envelope Designed to operate in the “reduced performance” conditions that were specified for the UT mount, but only for ambient temperatures above -15 degrees Celsius. Note: RD3 specifies an operating temperature range of -25 °C to +20 °C and a relative humidity of between 5% and 95%.

FLC-UR2-17: Space envelope Designed to fit onto Nasmyth table.

FLC-UR2-18: Cooling Designed to operate without an external supply of chilled water.

7.4 Design assumptions: FLC

It is assumed that FLC camera is of the same type as that chosen for the FTT/NA system. Consequently the constraints on protecting the camera from the environment are the same as for the FTT/NAS arrangement. There are two requirements that are different for the FLC system: one is that it must operate at an ambient temperature down to $-15\text{ }^{\circ}\text{C}$ and the other is that there is no requirement that the surface temperature of the camera enclosure be held to within $2\text{ }^{\circ}\text{C}$ of ambient.

A similar, if not identical enclosure will be used for the FLC camera. It may not be necessary to remove residual heat from the camera enclosure but it will be necessary to ensure that the camera internal air temperature does not fall below $0\text{ }^{\circ}\text{C}$ when operating or when it is called to operate. Dry air will still be needed to ensure that the camera can be operated when the ambient air is near the dew point.

7.5 Derived requirements: FLC

The camera enclosure air temperature must remain within the limits defined by the camera manufacturer:

1. Maximum enclosure internal air temperature: $30\text{ }^{\circ}\text{C}$
2. Minimum enclosure internal air temperature: $0\text{ }^{\circ}\text{C}$

To protect the camera from condensation forming in the enclosure the dew-point of the air within the enclosure should be $5\text{ }^{\circ}\text{C}$ below the coldest internal component.

3. Enclosure air dew point: coldest enclosure internal component $-5\text{ }^{\circ}\text{C}$

To respect requirement FLC-UR2-18 the residual camera heat must:

4. Residual camera heat $\leq 10\text{ W}$ [TBC] (based on likely temperature increase within camera enclosure without fluid cooling but excess heat may be extracted using the peltier chiller cooling loop).
5. A separate chilling unit must be used to remove heat from the peltier cooler within the camera if the telescope enclosure cooling system is not available at all times.

Dimensions of the camera enclosure are constrained to fit on the Nasmyth table consistent with the optical layout and the height restriction above the table.

6. Camera enclosure space envelope: arranged to fit potential layouts but no more than 350 mm high and nominally 340 mm wide and 300 mm deep.

The power requirements for the FLC are the same as those for the FTT/NAS:

7. CPU and interface power dissipation allowance 180 W
8. Camera interface and controller power dissipation allowance 64 W
9. Power consumption allowance 350 W but may require more if a separate chiller unit is required for the camera's Peltier cooler.

8 Closed-loop Bandwidth

In this section we derive the requirements on the camera latency implied by the top-level FTT closed-loop bandwidth requirement. The FLC will not do fast tip-tilt correction and so the results of this section do not apply.

8.1 Top-level requirements

The system is required to operate with a user-selectable closed-loop 3dB bandwidth in the range 10–40 Hz (adjusted according to the target brightnesses and seeing conditions). It is a goal that the system be capable of operating with a closed-loop 3dB bandwidth in the range 1–50 Hz.

8.2 Design assumptions

We assume a control loop consisting of a sensor, a controller and an actuator, and that the controller is a simple integrator, which ensures that the error tends to zero at low frequencies. For such a system, rules-of-thumb indicate that phase margins of 45 degrees give adequate robustness, i.e. the open loop phase change should be less than 135 degrees at 40 Hz (goal 50 Hz).

The controller uses 90 degrees of this phase change, and the FTTA has been specified to have no more than 20 degrees lag at 50 Hz, meaning that $135 - 90 - 20 = 25$ degrees of phase change is allowed in the “sensor”. This corresponds to a “sensor delay” of 1.73 milliseconds at 40 Hz bandwidth (1.39 ms for the 50 Hz goal).

The “sensor” delay is the total delay between a photon landing on the CCD and the corresponding correction command being sent to the actuator. This comprises:

- the “exposure lag” which is the time that the average photon sits on the chip if we could read the chip out instantaneously at the end of the exposure;
- the “readout latency” which is the delay from the end of exposure to the pixel data being available for processing; and
- the “compute latency” which is the time to do all the computations to go from pixel values to actuator commands.

We assume a frame rate of 1 kHz, which is achievable by the candidate EMCCD cameras using a custom subframe readout scheme. Hence the exposure lag is 500 microseconds – half the exposure time – for a frame transfer CCD. Note that the top-level bandwidth requirement could be satisfied at a lower frame rate but with a correspondingly shorter latency.

The compute latency can be calculated by assuming that any centroiding algorithm can be written as the product of a $3 \times N_{\text{pix}}$ matrix with a $1 \times N_{\text{pix}}$ vector to yield x and y centroids and the total flux (for normalisation). Hence we derive a total compute latency of 100 microseconds for a worst-case 32×32 pixel subframe. This is dominated by the time taken to transfer the pixel data and matrix coefficients from main memory to the CPU cache, the actual compute time being of order 3 microseconds for a 1 GHz processor. We have assumed a bandwidth to cache of 200 MB/sec. This is a conservative calculation because the matrix coefficients are likely to remain in the cache from one cycle to the next.

8.3 Derived requirements

Assigning the rest of the sensor delay to detector readout leads to a worst-case readout latency budget of $1730 - 500 - 100 = 1130$ microseconds for 40 Hz operation ($1390 - 500 - 100 = 790$ microseconds for 50 Hz).

9 Limiting Sensitivity

In this section we derive requirements on the noise performance of the FTT/NAS CCD camera from the top-level limiting magnitude requirement.

9.1 Top-level requirements

The FTT top-level requirement is an RMS residual two-axis tip-tilt < 0.060 arcsec for tip-tilt reference objects brighter than $V = 16$ in seeing conditions given by $r_0 > 14$ cm and $V_{\text{wind}} < 10$ m/s. The residual includes residual of the atmospheric disturbances, the Unit Telescope mount errors and the wind shake errors.

The FLC is only required to operate at 1–10 Hz frame rates on stars brighter than 10th magnitude, hence a camera that meets the derived requirements for the FTT will be more than adequate for the FLC.

9.2 Design assumptions

The frame rate and latency of the detector are assumed to be sufficient that the system can be analysed as a continuous-time servo. We assume the use of an E2V CCD97 operated in “analogue” i.e. non-photon-counting mode in a camera with a window whose transmission is that given for Princeton Instruments’ VISAR coating. The telescope is assumed to have a throughput as given by the combination of the reflectances of aluminium and silver surfaces measured on the witness samples from OST minus the 5% obscuration due to the secondary and the telescope spiders. The atmosphere is assumed to have an atmospheric transmission which is somewhat pessimistic, with a value close to that for Palomar observatory, which is at a lower altitude and so should have poorer transmission.

9.3 Derived requirements

The overall tilt error budget is given in Table 4.

Tilt error	RMS error (milliarcsec)
UT residual mount error	20
UT residual wind shake	30
Residual seeing tilt	30
Speckle noise centroiding error	15
Detection noise centroiding error	34
Total	60

Table 4: The two-axis tip/tilt error budget in seeing conditions of $r_0 = 14\text{cm}$ and $V = 10$ m/s

The residual UT jitter values are taken from the UTM Requirements Document assume a servo bandwidth of 10 Hz, but the optimal servo bandwidth for the faint-object and good-seeing scenario given in the FTT requirement is approximately 15 Hz. Thus the values used are upper limits.

Tyler [1994] gives a formula for the one-axis residual tilt fluctuations from a first-order servo as

$$\sigma_t = \left(\frac{f_T}{f_{3\text{dB}}} \right) \left(\frac{\lambda}{D} \right) \quad (1)$$

where $f_{3\text{dB}}$ is the servo cut-off frequency, λ is the mean wavelength sensed by the tip/tilt detector, D is the diameter of the telescope. For “Zernike tilt” then the Tyler frequency is given by:

$$f_T = 0.368 \frac{D}{\lambda} \left[\int C_n^2(h) |V(h)|^2 dz \right]^{1/2}$$

where C_n^2 is the seeing strength and $V(h)$ is the wind velocity at height h . For constant wind velocity with height V_0 then

$$f_T = \frac{0.09005V_0}{D^{1/6}r_0(\lambda)^{5/6}} \quad (2)$$

Combining equations 1 and 2 and multiplying by $\sqrt{2}$ to convert from a 1-axis error to a 2-axis error gives the value in Table 4.

The speckle noise centroiding error can be estimated from considering the ‘‘centroid anisoplanatism’’ [Sasiela and Shelton, 1993] which is the difference between the centroid given by ‘‘centre of mass’’ centroid algorithms (known as ‘‘G-tilt’’) and the Zernike tilt mode (‘‘Z-tilt’’) caused by higher-order atmospheric modes such as coma. Different centroiding algorithms give quite different amounts of error as shown by Tokovinin [2002], although he did not model seeing conditions appropriate for the scenario considered here. The value chosen is an intermediate one between that for conventional centre of mass algorithms and that for thresholded centre of mass algorithms. This number needs to be checked against simulations of more realistic seeing conditions and different centroiding algorithms e.g. quad-cell.

The two-axis detection noise centroiding error for a quad cell is given by [Olivier and Gavel, 1994]:

$$\sigma_d = \sqrt{\frac{2\pi f_{3dB}}{f_s} \frac{1}{\text{SNR}} \frac{3\pi\lambda}{16kD}}$$

where k is an image quality degradation measure relevant to quad-cell centroiding and SNR is the per-frame signal-to-noise ratio for the detection of total flux. EMCCD multiplication noise results in a doubling of the noise variance compared to that due to the photon noise alone, so that the SNR is given by

$$\text{SNR} = \frac{N}{\sqrt{2N + n\sigma_r^2}} \quad (3)$$

where N is the number of detected photons per frame (before electron multiplication), n is the number of pixel reads and σ_r is the effective read noise referred to the input of the electron-multiplying register. Assuming for the moment that the read noise is negligible, we have

$$\sigma = \sqrt{\frac{4\pi f_{3dB}}{N_g} \frac{3\pi\lambda}{16kD}} \quad (4)$$

where $N_g = f_s N$ is the number of detected photons per second. Note that the centroiding error is not dependent on f_s under the assumptions of no read noise and fast sampling.

For $\lambda \sim 500$ nm, $r_0(\lambda) = 14$ cm and $D = 1.4$ m then $\frac{\lambda}{kD} \approx 0.49$ arcsec [Buscher, 1988, Figure 5.8], after allowing for a 10% degradation due to imperfect optical quality. This angle is not a strong function of the assumed centre wavelength, since k increases approximately linearly with λ for $D \gg r_0$.

Solving equation 4 for N_g gives a value of 13,644 photons/sec needed to reach the centroiding error budget requirement. When using a dichroic that reflects all of the light from 600nm-1000nm, then the camera would detect 13,402 photons/second from a 16th magnitude star of the colour described in the requirements if there were 100% throughput from the telescope to the camera entrance window.

This means that, even without accounting for losses due to the FTT optics, the system cannot meet the faint source centroiding requirement. However, even including losses in the FTT optics of perhaps 15% would mean that the total residual tilt is only some 2% over budget. This would result in an additional visibility loss in the H-band of approximately 0.5% over what has been budgeted. Some of this performance could be regained if the telescope jitter is primarily at low frequencies: in this case the 15 Hz bandwidth used in the tip/tilt servo instead of the 10 Hz bandwidth used in the UTM specification would result in approximately 33% reduction in the RMS residual tilts from each of the UT tilt error sources. Use of different centroiding algorithms, e.g. correlation algorithms may result in lower centroiding errors at these light levels and help to reduce the overall residual.

We now need to estimate the level of read noise which makes the assumption of negligible read noise appropriate. For the purposes of this we will assume that the read noise is negligible if the centroiding accuracy is decreased by less 1% by the read noise when compared with the no-read-noise case. For the worst-case throughput and a frame rate of $20f_{3dB}$, then the number of photons detected per frame is $N = 13402 \times 0.85/300 = 38$. Referring to equation 3 it can be seen that we need an effective read noise of $\sigma_r < 0.20$ electrons to meet the above criterion if $n = 36$ corresponding to a 6×6 pixel quad cell. This implies electron multiplication gains of at least 250 for an EMCCD system with an output read noise of 50 electrons.

10 Dynamic Range

This section presents derived requirements on the FTT/NAS and FLC related to their capability to observe both bright and faint stars.

10.1 Top-level requirements

There is no top-level requirement setting the brightest stars to be observed, for either the FLC or FTT/NAS. The faintest star requirements for the FTT are set out in the section on “limiting sensitivity”. The limiting magnitude for the NAS is the same as that for the FTT. The faint star requirement for the FLC is that it should be able to operate with stars as faint as $V = 10$, assuming an A spectral type.

10.2 Design assumptions

We shall assume a goal that the system should be capable of observing the brightest objects which are scientifically interesting. These are typically red supergiants of which Betelgeuse is the brightest candidate: it has a colour similar to that of the required faintest star, but a V-magnitude of approximately 0.5.

It is assumed that an E2V EMCCD is used and that the unamplified readout has a read noise of 50 electrons RMS.

It is assumed that, for the FTT mode, the EMCCD gain should be changed as infrequently as possible so that any background-level calibrations of the CCD need to be done as infrequently as possible. Similarly we assume that the frame rate is kept the same wherever possible without sacrificing other requirements, so that any effects on interferometric visibility resulting from changes in control loop latency are minimised. We assume that by default the frame rate will be the maximum frame rate of 1kHz except for the very faintest stars.

For the NAS mode and the FLC, it is assumed that the camera is always read out full-frame. Since the frames are large enough that the majority of pixels will be sky background, we assume that the background levels can-be determined on a frame-by-frame basis. As a result, there is no need to keep the same exposure time or EMCCD gain for background calibration purposes.

It is assumed that in the FLC and NAS modes the exposure time can be adjusted independently of the frame rate and that the minimum exposure time is 1 millisecond.

10.3 Derived requirements: FTT

The faint star limit has been addressed in the section on “limiting sensitivity”. If the optical system has the lowest acceptable throughput to reach the faint star requirement then 19×10^9 photons per second will be detected when observing Betelgeuse. At a frame rate of 1 kHz and assuming a FWHM of 3 pixels (the “worst case” which occurs in the best seeing), then the peak number of photons per pixel per frame is approximately 2.1×10^6 . The pixel well depth is 160,000 electrons so the central pixels of the tip/tilt sensor will be saturated.

It may be possible to centroid on outer pixels in the image as long as the saturation does not cause excessive “bleeding” of charge from the central pixels to outer pixels. An alternative is to reduce the number of photons hitting the FTT sensor, using e.g. a pupil mask or neutral density filters.

Without the use of such options, the brightest star of this type observable in the worst case would have a V magnitude of 3.3, which leaves a large number of supergiants available for study: these would also be more favourable from the point of view of not being over-resolved by the interferometer baseline. The problem of saturation is much reduced in worse seeing: for seeing which is a factor of 2 worse, sources some 1.5 magnitudes brighter can be observed.

At the maximum EMCCD gain used at low light levels (gain of 250) the equivalent well depth is limited by the 800,000-electron well depth of the amplification register. This corresponds to 3,200 photons per pixel per frame, which means that brightest object observable at this gain setting has a magnitude of $V = 7.5$.

A conservative estimate of the faintest object observable when there is no amplification can be obtained by considering when the SNR per pixel per frame when considering read noise alone falls below 10. For a read noise of 50 electrons this occurs when the photon rate is 500 photons per pixel per frame, which means that there is a 2-magnitude overlap between the faintest objects observable without amplification and the brightest objects observable with amplification. Thus only 2 gain settings are needed in principle to cover the complete magnitude range.

11 Derived requirements: NAS and FLC

If the minimum exposure time in the NAS and FLC modes is 1 millisecond, then the brightest stars observable without saturation are the same as for the FTT mode. If we assume that the camera is operated without amplification in NAS and FLC modes, then the faintest stars observable are set by the 500 photon-per-pixel-per-frame limit given in the previous subsection. At 1 millisecond sample time and in the best seeing, then the magnitude limit would be $V = 9.5$. Thus to reach the faint-source requirements for the FLC and NAS in seeing twice as bad as the best seeing, then exposure times of greater than 6 milliseconds and 1.6 seconds are required respectively.

The latter exposure time is not consistent with frame rates of 1Hz or faster required for rapid acquisition, so some EMCCD gain would be preferred for the NAS when acquiring stars fainter than about $V = 15$ in poor seeing, though it should be noted that the FTT mode would not work well with faint sources in such seeing. Using the same set of gain settings as for the FTT would minimise the number of gain settings which would need to be tested, and would clearly be more than adequate to meet the dynamic range requirements.

References

- David Buscher. *Getting the most out of COAST*. PhD thesis, University of Cambridge, 1988.
- S. S. Olivier and D. T. Gavel. Tip-tilt compensation for astronomical imaging. *Journal of the Optical Society of America A*, 11:368–378, January 1994. URL <http://adsabs.harvard.edu/abs/1994JOSAA..11..368O>.
- Francois Roddier, Malcolm Northcott, and J. Elon Graves. A simple low-order adaptive optics system for near-infrared applications. *Publications of the Astronomical Society of the Pacific*, 103:131–149, January 1991. URL <http://adsabs.harvard.edu/abs/1991PASP..103..131R>.
- Richard J. Sasiela and John D. Shelton. Transverse spectral filtering and mellin transform techniques applied to the effect of outer scale on tilt and tilt anisoplanatism. *Journal of the Optical Society of America A*, 10: 646–660, April 1993. URL <http://adsabs.harvard.edu/abs/1993JOSAA..10..646S>.

- A. Tokovinin. From differential image motion to seeing. *Publications of the Astronomical Society of the Pacific*, 114:1156–1166, October 2002. URL <http://adsabs.harvard.edu/abs/2002PASP..114.1156T>.
- Glenn A. Tyler. Bandwidth considerations for tracking through turbulence. *Journal of the Optical Society of America A*, 11(1):358–367, January 1994. doi: 10.1364/JOSAA.11.000358. URL <http://josaa.osa.org/abstract.cfm?URI=josaa-11-1-358>.